Chapter 6

Mechanical Perturbations at the Working Electrode to Materials Synthesis by Electrodeposition

Baudel Lara Lara, Arturo Fernández Madrigal,
Lizbeth Morales Salas and
Alejandro Altamirano Gutiérrez

Additional information is available at the end of the chapter

http://dx.doi.org/10.5772/intechopen.78544

Abstract

Applying mechanical perturbations at the working electrode during the electrodeposition process is a novel strategy for materials synthesis that has been used for Cu(In,Ga)Se_2 (CIGS) thin film synthesis. A mechanical perturbations strategy was applied during one-step electrodeposition, and the results are compared with the traditional one-step electrodeposition where no mechanical perturbations were applied. In both cases, a potentiostatic mode was employed, where DC potential is applied to the working electrode with respect to the reference electrode; the potential is regulated by the current at an auxiliary electrode. The CIGS films obtained from both strategies were analyzed as electrodeposited and after being annealed in a selenium atmosphere. The annealed film morphology obtained with the potentiostatic mode plus periodical mechanical perturbations was denser and more compact than the film without mechanical perturbations. Using contour lines, the morphology evolution and mass transport distribution on the working electrode during the electrodeposition process are explained.

Keywords: mechanical perturbations, electrodeposition, thin film, morphology

1. Introduction

Advance of new materials is an important issue in different areas of the technological development; however, the challenges are still diverse and important. A necessary aspect of human survival is the use of renewable energies, especially the solar energy. A technology that can convert the solar radiation in electricity directly is the use of solar cells. Different methods for

materials synthesis have been widely investigated for solar energy conversion. These methods can be classified into physical and chemical. Electrodeposition is a chemical method that has been used to obtain metallic or semiconducting films on substrates, with the aim of protecting the surface against the oxidation and corrosion, giving a better esthetic appearance, and providing some mechanical and electrical characteristics, different to the base material, to improve its physical properties. Electrodeposition has been considered for solar cell applications for a long time [1], with a considerable potential for the fabrication of a low-cost thin film for solar cells [2]. It is simple, versatile, and economical as compared to physical methods, such as high vacuum processes. Some of its advantages are requiring less capital investment, saving raw material, application on irregular surfaces, and industry scalability potential. It has been used for materials synthesis for perovskite [3], Cu_2ZnSnS_4 [4], and $CuIn_xGa_{(1-x)}Se_2$ (CIGS) solar cell [5]. It is also used for nanoparticle synthesis for solar collectors [6] and to develop technology in the energy storage [7].

The electrodeposition method is considered difficult; perhaps because the electrodeposition process is affected by many variables. Some of them are concentration of the solution, solution temperature, pH, working electrode potential, working electrode resistivity, and distance between electrodes. During the electrodeposition process, there are phenomena that affect the film growth, among them, the diffusion layer, the depletion region, and the natural flow by convection. For such reasons, the electrodeposition method is still under investigation to improve the material quality.

2. Conventional electrodeposition

A conventional three-electrode electrolytic cell connected to potentiostat equipment is used for material synthesis investigation in solar cell applications by electrodeposition. A direct current (DC) potential is applied to the working electrode (WE) with respect to the reference electrode (RE). The DC potential in the WE is regulated in a closed-loop control system by adjusting the current at an auxiliary electrode (AE). According to the electrolytic solution, different materials can be deposited on the WE. Synthesizing a material by the electrodeposition technique consists of finding the values of the variables that produce a film growth with the desired characteristics. Thin films of materials with homogeneous growth and compact morphology are desirable. If the material to be formed consists of two or more elements, there are diverse electrodeposition alternatives, principally (1) electrodeposition of elements in layers, followed by annealing, to get the desired structure, and (2) electrodeposition of elements in a simultaneous way, also followed by annealing, to increase crystallinity. The latter alternative is known as a one-step electrodeposition in which the electrochemical conditions must be met in such a way that the material composition is homogeneous from the first instant of formation. The advantage of the one-step electrodeposition alternative is that the film that is obtained is electro-crystallized. In addition, a single electrolytic solution with ions of the precursor elements is used, while in the electrodeposition by layers, an electrolytic solution is used for each layer.

The basic modes of crystal growth on a WE under electrochemical conditions have been established; the electrodeposition takes place at the electrode-electrolyte interface under the

influence of an electric field [8]. A scheme of load distribution as well as a simple electrical model of a three-electrode electrolytic cell is represented in **Figure 1**. Charge distribution in the electrode-electrolyte interface is analogous to charge distribution in a capacitor which is called the electrical double layer. The electric field lines are defined only at the interface, where C_{WE} and C_{AE} are the equivalent capacitances between the WE and AE and the solution, respectively. R_{SOL} is the solution electric resistance. In a three-electrode-electrolytic cell, the electrode-solution interface is principally important in the WE and AE. Other detailed electric models [9] for the electrode-solution interface suggest that the interface is affected by the capacitance of the double layer, the resistance in the charge transfer zone, and the impedance due to adsorption and mass transport, and the parameter of the electrical model, mentioned earlier, can be obtained by electrochemical impedance [10].

In an electrodeposition process, the charge, which consists of electrons, is considered to be evenly distributed on the WE surface. When M^{2+} ions are present in the solution, the electrochemical of $M^{2+} + 2e \rightarrow M$ is carrier out on the WE. When more than one type of ions must be reduced, the transport mechanism of the ions until the load transfer zone plays an important role. It is assumed that the ratio at which the ions are consumed by the charge transfer reaction is equal to the ratio at which the ions arrive at the charge transfer zone.

At the beginning of the electrodeposition process, the first nuclei grow on the WE surface. At that time, the solution around the nuclei is depleted of ionic species, and the only factor that influences the ion movement is diffusion [11], through which the depleted zones around the

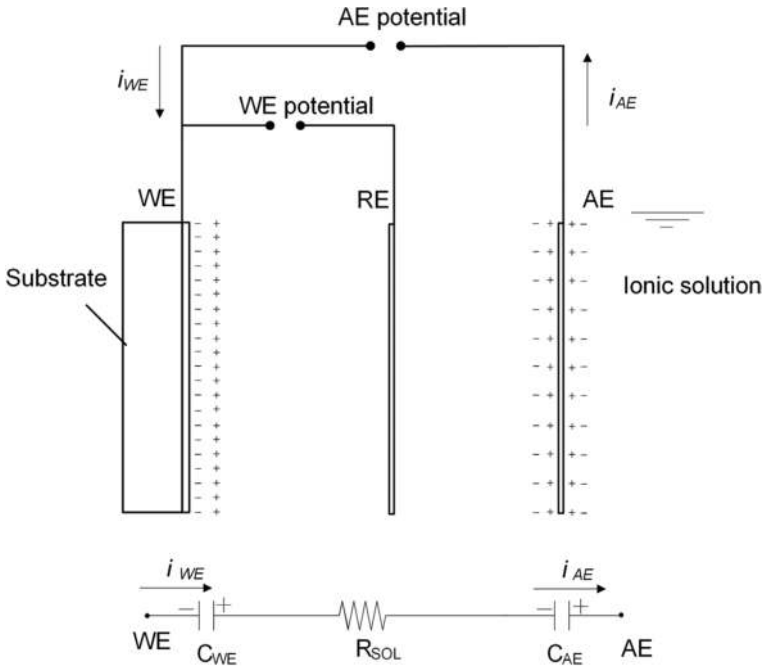

Figure 1. A diagram of a simple electrical model of a three-electrode electrolytic cell.

nuclei start to propagate throughout the WE surface; as the electrodeposition time elapses, these zones begin to overlap [12]. **Figure 2** shows a schematic representation of the ion movement distribution on the WE surface at the initial stage of the film formation. The arrow lines

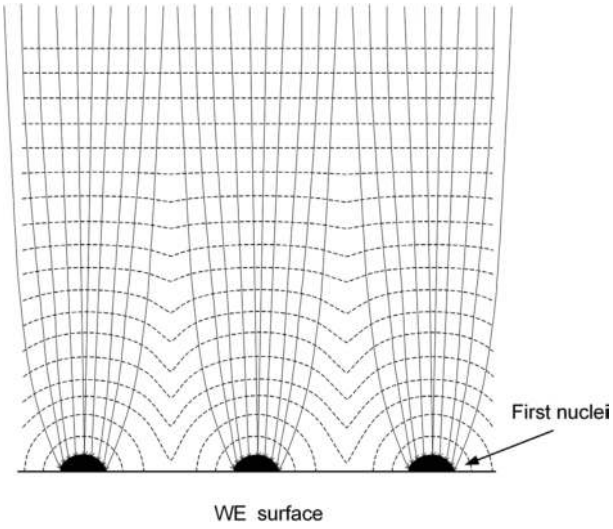

Figure 2. A schematic representation of the mass transport distribution at the initial stage of the film formation by electrodeposition (modified from [12]).

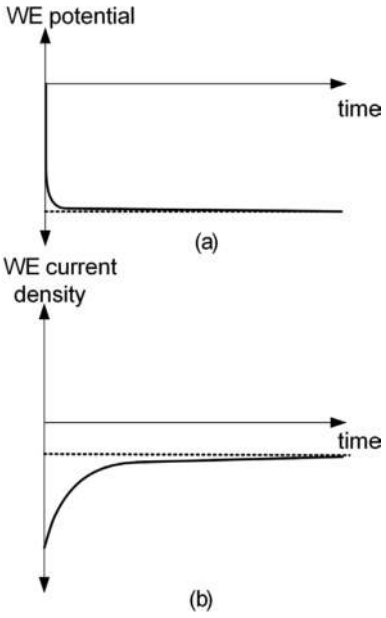

Figure 3. A graphic representation of electrodeposition signals versus time obtained during the electrodeposition process: (a) WE potential and (b) WE current density [13].

show the ion movement from the bulk solution to the WE vicinity. In this region, the ions concentration is different from their value in the bulk solution; this region is known as the diffusion layer.

When the DC potential is applied at the WE, the current density versus time shows a transitory stage evolution, followed by a stage where the current variation is lower than the transitory stage. Also, the potential has a transitory stage; after that, the WE potential reaches the set value. With acquisition data software, the voltage and current signals can be plotted as time function, as it is shown in the graph in **Figure 3**. According to the above, the electric model of the three-electrode-electrolytic cell represents an average model of the electrical phenomena that take place in the electrode-solution interface during the electrodeposition process.

3. CIGS thin film by electrodeposition

The semiconductor CIGS is a promising absorber in thin film solar cells, due to their direct band gap and large optical absorption coefficient. Small-area CIGS solar cells with efficiencies reaching 22.6% have been built with this semiconductor synthesized by the high vacuum deposition method [14]. A compact absorber morphology is a quality indicator to obtain high performance CIGS solar cells. To improve solar cell efficiency, the CIGS absorber should have, in cross view, large grains extending from the back to the front [15]. The CIGS absorber has the highest potential to develop large-scale solar cells. Employing high vacuum deposition method, high efficiencies have been achieved; however, economical deposition methods with the possibility of implementing in large area still need to be developed [16, 17]. It is considered that the CIGS absorber can be synthesized in a large area and with compact morphology employing the electrodeposition method. However, when CIGS solar cells have been built by synthesizing the absorber by electrodeposition, solar cell efficiencies of 11.3% for a one-step electrodeposition [18] and 14.17% for layers electrodeposition [19] have been achieved. The low efficiency is attributed to lack of absorber quality when it is obtained by the electrodeposition method, usually associated with the morphology. Microcracks have been identified in the CIGS film obtained by a one-step electrodeposition [20], which is one reason why relatively low efficiencies are obtained in the CIGS solar cell by electrodeposition.

To develop the CIGS solar cells on a large scale by electrodeposition, there are still aspects that must be investigated. The major challenges and required strategies have been identified. Among them, (1) the precise control of film stoichiometry (optimization of Ga content and Ga distribution), (2) novel deposition strategies, (3) understanding on the mechanism of Ga incorporation, and (4) establishing the strategy that allows electrodepositing the semiconductor with homogeneous composition and uniform morphology throughout the film [16, 21].

In several works, electrodeposition strategies for thin films synthesis have been used. It has been established that by using a pH-regulating solution, stability is provided to the electrodeposition process. No oxides or hydroxides are obtained in the solution, and it is possible to incorporate a higher percentage of gallium in the film [20]. In the first stages of Cu-In-Se on Mo-coated glass by electrochemical deposition, the first nuclei are made of a copper-rich Cu-Se without indium and the nucleation is developed by a quasi-instantaneous three-dimensional

nucleation [22]. In $CuInSe_2$ (CIS) one-step electrodeposition, it has been established that the Cu-Se phase is formed at a low potential, and a reaction path has been established as a function of the potential. The Cu-Se phase acts as a nucleation site for indium incorporation [23, 24]. The CIS film morphology deposited at various potentials has been analyzed [23]. At low polarizations between −0.4 and − 0.5 V, platelets characteristic of the Cu-Se were observed; when the polarization increased, the morphology was nodular. The mechanisms of Ga to CIS incorporation also have been established. It is incorporated as gallium selenide and GaO_3 [25]. The CIGS film morphology obtained by the one-step electrodeposition with potentiostat mode has been described as nodules with a cauliflower-like growth [22, 26]. The as-electrodeposited CIGS film morphology is strongly influenced by the bath composition. Microcracks in the films have been observed when the films were deposited at low concentrations of $CuCl_3$, $InCl_3$, and $GaCl_3$ salts and at high concentrations of H_2SeO_3 [27].

Many studies have examined ways of improving the CIGS film morphology by a one-step electrodeposition. The effect of sodium sulfamate as a complexing agent on the film morphology was evaluated [28]. An improvement on CIGS thin film morphology was obtained when a short electrode pretreatment of a 1-min deposition at −0.5 V was carried out prior to deposition of the film [29]. The pulse electrodeposition process can produce a CIGS film that is more smooth, compact, and homogeneous than the one deposited by the DC potential electrodeposition [30]. Electrochemical studies in CIGS electrodeposition, generally, use an electrochemical cell with electrodes suspended vertically. However, an electrochemical cell with electrodes in a horizontal position has advantages over a cell with vertical electrodes, principally because the ion transport mechanism as well as the natural flow by convection allows a better uniformity on the WE surface; in this way, the composition is homogeneous through the film [31].

3.1. Characterization of CIGS films obtained by electrodeposition

An electrochemical cell system of three horizontal electrodes was installed with a scheme like the one shown in **Figure 4**. A glass substrate covered by an Mo film (1 μm of thickness and $4x10^{-4}$ Ω cm of resistivity) was the WE. The RE and AE were made of a platinum mesh. The CIGS films were electrodeposited by applying −1.0-V DC potential to the WE versus the RE, employing an electrolytic solution with copper, indium, gallium, and selenium ions. At the start, it was the electrodeposition process, where a stage of nucleation and electrocrystallization of the CIGS film on the WE electrode was obtained. After the electrodeposition process, the WE with the CIGS film was removed from the electrochemical bath, rinsed with deionized water, and placed vertically for drying. Although copper, indium, gallium, and selenium ions have different reduction potential, a situation that complicates a simultaneous ED process, the CIGS films have been obtained with the composition ratios of Ga/(In+Ga) = 0.31 and Cu/(In+Ga) ≈ 0.9, close to those reported in the high efficiency cells [32, 33]. The film composition was measured by atomic emission spectroscopy (ICP-AES). The current evolution indicates that the steady-state value can be reached after 5 min, with a limiting current density of ≈ 1 mA / cm^2. The WE surface changes during the film formation affect the limiting current density in the steady state in such a way that it decreases with very slow dynamics. The above also indicates that diffusion layer thickness increases. During the steady stage, the reaction at the WE is affected by the

http://dx.doi.org/10.5772/intechopen.78544

transport of the chemical species from the bulk solution to the charge transfer zone. By increasing the electrodeposition time, the film obtained is more rugged and darker in color; this is due to the lack of ions near to WE and to the increase of the diffusion layer thickness. The stirring of the solution is desirable since it enhances ion transport to the substrate and decreases the thickness of the diffusion layer [34]. However, the agitation method of stirring for a laboratory-scale deposition leads to gradients of thickness in the flow direction of the electrolyte [35].

The CIGS films characterized by scanning electron microscope (SEM) are shown in **Figure 5**. **Figure 5(a, b)** shows micrographs of surface and cross section. In both cases, the morphology consists of vertical nodules with a well-defined boundary between them. Some nodules are larger than others, which apparently have stopped growing. The stunted nodules increase the boundary between the nodules that have a greater growth. **Figure 5(c)** shows the surface morphology of the vertical nodules with a cauliflower-like growth. The surface morphology among the nodule boundaries is shown in **Figure 5(d)**. The film morphology in the nodule has differences with the one that exists in the boundary. Apparently, the film formed between boundaries is less compact than those formed in the nodule. In general, the CIGS films that were obtained through the one-step electrodeposition are not very compact and have a low crystalline structure, so that they do not have the properties to be used in solar cells. The principal morphology consisted in groups of atoms forming the cauliflower-like growth. The annealing process in a selenium atmosphere is necessary to transform the as-electrodeposited film into a more crystalline, with large grains and with compact morphology.

The CIGS thin films that were subjected to an annealing process in a selenium atmosphere are shown in **Figure 6**. The selenization temperature was 550°C for 180 min. **Figure 6(a,b)** shows the surface and cross-section micrographs. In the micrographs, there is evidence that the nodules are of different length. On increasing the deposition time, some nodules continue

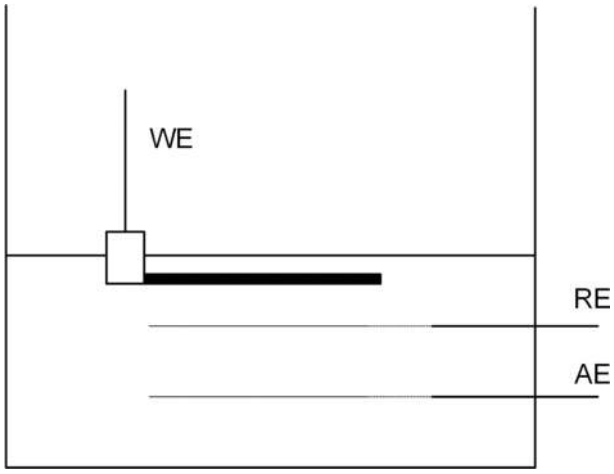

Figure 4. A diagram of an electrolytic cell with three horizontal electrodes.

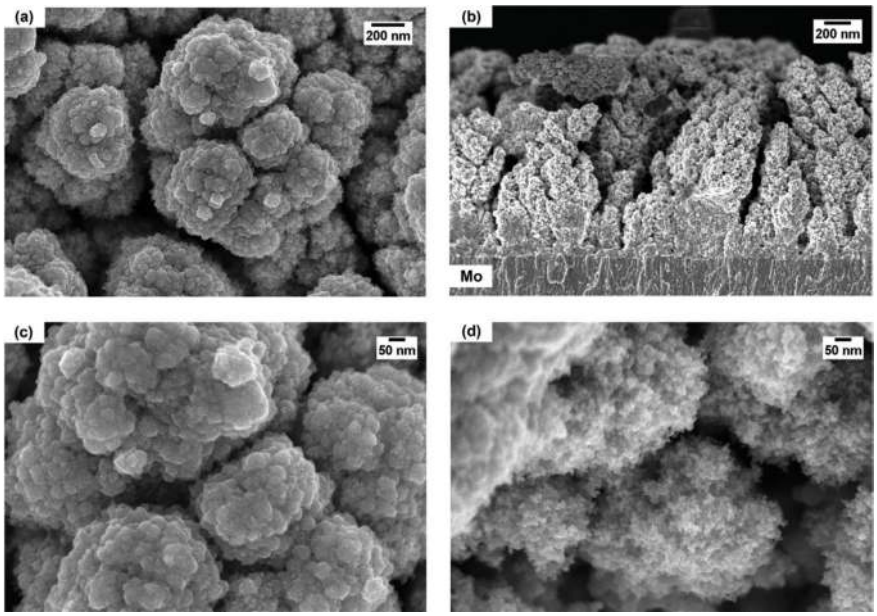

Figure 5. Micrographs of the CIGS film that has been electrodeposited in a conventional mode: (a) surface, (b) cross section, (c) nodule with a cauliflower-like growth, and (d) morphology in the nodule boundary [13].

to grow and others stop growing. The cross-section film micrograph shows the Mo layer and over it, a CIGS film with a compact morphology with 300 nm of thickness; this layer is also evident from the as-electrodeposited film shown in **Figure 5(b)**. It was noticeable that the compact layer is due to the initial growth when the current density is in a transitory state and the diffusion layer is thin. Over the compact CIGS film, there are only formations of isolated nodules of different sizes with very large boundaries between them; in this stage of formation, the current density and the mechanism of mass transport are not locally uniform. In order to reduce the activation energy and grow large grains during the annealing process, a Cu-rich film was prepared. The film composition ratios were Ga/(In+Ga) = 0.29 and Cu/(In+Ga) = 1.18. The Cu content of the film determines the activation energy for grain boundary motion. It has been determined that by increasing the Cu content of the film from 17.9 to 25.7%, the activation energy decreases from 3.5 to 3.0 eV [36]. The micrographs of annealed films are shown in **Figure 6(c, d)**. From these micrographs, it can be noted that there is also a compact CIGS film over the Mo film, which shows that in the copper-poor and copper-rich films, the films are compact in the first stage of growth, up to a thickness of 300 nm. A nonuniform grain growth is identified. There is only a grain growth in the boundaries indicating that the kinetic of grain growth during selenization process in the nodule boundaries was different, which is believed to be caused by the non-homogeneity in the film composition originated by the nonuniformity of the current density during the one-step electrodeposition process. Copper-rich films were formed in the nodule boundaries. In this way, the atomic composition in the films is not uniform, the nodules are copper-poor, and the boundary nodules are copper-rich. That is, the film locally will have different electrical, structural, and optical characteristics.

http://dx.doi.org/10.5772/intechopen.78544

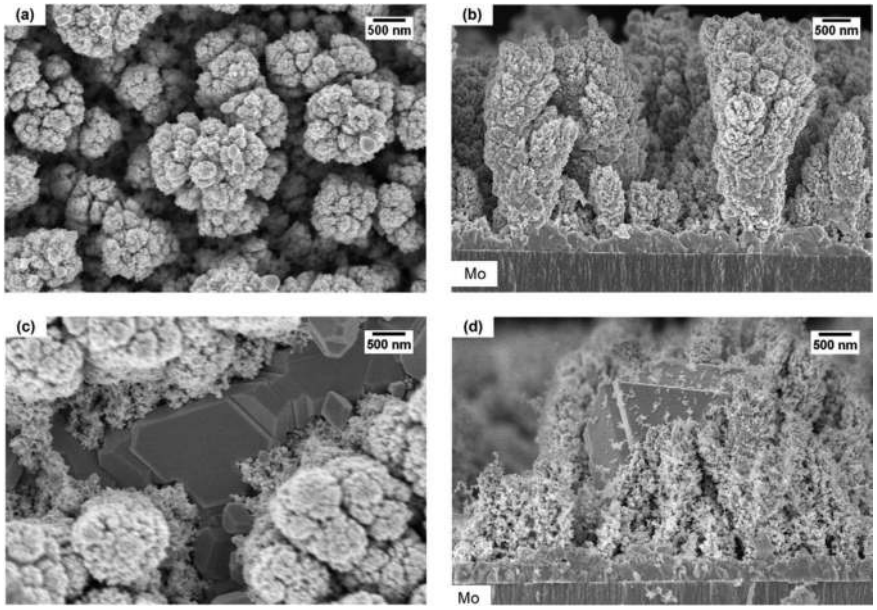

Figure 6. Micrographs of surface and cross section of the CIGS films with (a, b) composition ratio Cu/(In + Ga) = 0.9 and (c, d) composition ratio Cu/(In + Ga) = 1.18 [13].

4. Conventional electrodeposition plus periodical perturbations

In the electrodeposition theory, it is assumed that the WE surface is homogeneous so that the current density in the macroscopic level is uniformly distributed over the WE surface [8]. However, at the microscopic level, if the surface of the WE is considered as a surface with roughness, there will be a greater electric field strength in the peaks than in the surface valleys, as shown in **Figure 7(a)**, where the WE roughness has been amplified. Thus, the electrochemical kinetic is affected. For this reason, the electric load will be concentrated in the crests of the WE. With the formation of the first nodules, the WE roughness increases in such a way that the current density and therefore the mass transport mechanism are concentrated at the nodules. The foregoing has been observed in other studies, where it has been determined that the nonuniformity in the local current densities can exist even when the macroscopic current distribution over a given surface is completely uniform [34]. Assuming that there is a direct relationship between the load transfer ratio and the current density that is demanded during the electrodeposition process, the load transfer process can be analyzed using the current density. The points of greatest intensity of the electric field are the crests of the WE. In this way, they produce a greater current density during the ion reduction process, in such a way that, in the crests, the growth of the film originates grains that grow perpendicularly with respect to the WE. In the valleys, the current density is lower, and therefore, the density of ions is reduced and the growth speed of the film is slower. From the previous results, it can be established that as a consequence of nonuniformity in the local current densities through the WE, due to the diffusion layer growth, the CIGS morphology consists of isolated nodules

with a cauliflower-like growth. It is evident after the transitory stage in the electrodeposition current density, and this is more noticeable when the electrodeposition time increases, a representation of isolated nodules is shown in **Figure 7(b)**.

The contour lines are used in topographic maps to represent points of the same elevation. Here, we use it to represent the CIGS film morphology as shown in **Figure 8**. The contour lines were traced according to the film morphology shown in **Figures 5** and **6**. The contour lines represent the CIGS film morphology of the same thickness. According to the micrographs, the CIGS films morphology is not uniform through the WE surface, being a function of the current density distribution during the electrodeposition process. Thus, the contour lines also represent the mass transport mechanism during the electrodeposition process. **Figure 8** shows the contour lines that represent the electrodeposition process evolution. The highest mass transport density and the nodule formation are represented in zones with a dark color while less mass transport density and the boundary layer formation between nodules are represented with a light gray color. When the electrodeposition process begins, a large number of nodules grow randomly distributed. The nodules distributions, which can be appreciated after the current transitory stage, are represented in **Figure 8(a)**. When the first nodule has a cauliflower-like growth, the mass transport mechanism is concentrated in them; however, not all nodules grow at the same rate and eventually some stop growing. When the deposition time elapses, the nodules become more and more isolated and the boundary between them grows, because the mass transport mechanism is concentrated at very isolated points; this is represented as contour lines in **Figure 8(b, c)**. The above causes the CIGS film morphology to appear as isolated nodules with a high roughness, and this is evident when the electrodeposition time increases. In previous studies, it has been shown that in the CIGS film synthesized by electrodeposition, the composition is related to the current density; if

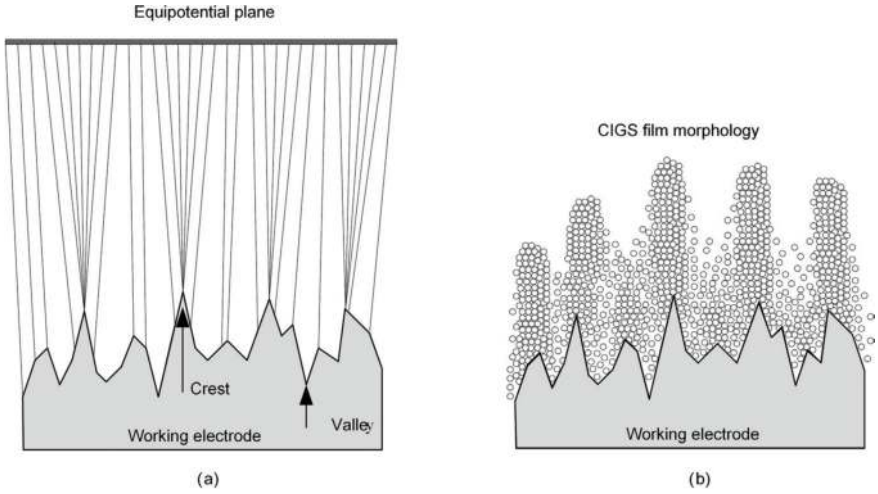

Figure 7. Growth model of CIGS films, obtained by the one-step electrodeposition: (a) effect of the WE roughness on the distribution of the electric field and (b) effect of the distribution of the electric field on the film morphology.

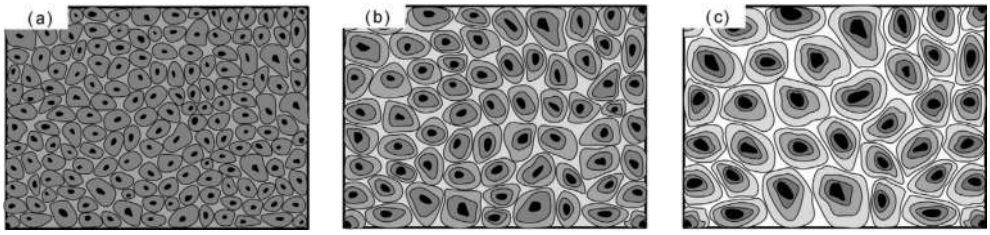

Figure 8. Contour lines that represent the CIGS film morphology, mass transport, and current density distribution in three different stages of the electrodeposition process [13].

the current density is high, the CIGS film composition is copper-poor. On the other hand, if the current density is low, the CIGS film composition is copper-rich [31]. Therefore, the CIGS film has a composition that varies according to the contour line; the zones with a dark color are cooper-poor while the zones with a light gray color are copper-rich. The above is evident in the surface morphology of CIGS films that were subjected to an annealing process as shown in **Figure 6(c, d)**. At the initial stage of the electrodeposition process, the ratio of ion reduction in the WE surface is much greater than the speed at which the ionic species arrive at the load transfer zone; for this reason, the diffusion layer increases up to maintain an electric load balance. In this way, the zone of the depletion varies according to the contour plot. At this microscopic level, the diffusion layer is not uniform along the working electrode. It acquired this principal shape after the transient of the electrodeposition current density. At the macroscopic level, experimental results [37] revealed that the electrochemical kinetic behavior of CIGS thin films is strongly influenced by the electrical double layer existing between the substrate. With an increase in the electrodeposition time, the kinetic behavior of this electrodeposition system was gradually dominated by the diffusion process rather than charge transfer process.

5. CIGS thin film by electrodeposition plus periodical mechanical perturbations

The strategy of applying mechanical perturbations to the WE during the electrodeposition process was the result of analyzing the morphology of CIGS film produced by electrodeposition using DC potential at the WE; details of film preparation can be found in [13]. As it was shown with the cross-section micrographs, during the initial stage of CIGS film growth, a more compact CIGS layer is produced. This is evident in the as-electrodeposited film and in the annealed film. In order to promote this formation, a mechanical perturbation to the working electrode was applied every 0.066 C/cm^2 during the electrodeposition processes. With the mechanical perturbation, the solution near the WE, producing perhaps turbulent flow, the diffusion layer tends to disappear for a moment and a new nucleation and growth center was originated, and if the perturbation is periodical, the film will be more compact.

Figure 9(a, b) shows the typical signal of the WE potential and current density versus time collected during the electrodeposition process by applying periodical mechanical perturbations to the WE. The average current density value was 2.4 mA/cm^2. The WE potential and the current density were periodically related to the periodicity of the mechanical perturbations. The WE potential had a variation of −1.0 to −0.995 V at each mechanical perturbation. With the periodical mechanical perturbations, it was possible to make CIGS films with 1.2–1.5 μm in 20 min, and the growth was faster with respect to not using mechanical perturbations. The film composition rations were of Ga/(In+Ga) = 0.28 and Cu/(In+Ga) = 0.93. With the mechanical perturbations, no film dissolution was produced as is presented in pulse reverse electrodeposition.

5.1. Characterization of CIGS films obtained by electrodeposition plus mechanical perturbations

The surface and cross-section morphology of the as-electrodeposited CIGS film are shown in **Figure 10(a, b)**. It is identified that by applying mechanical perturbations, the films are more compact and with less roughness compared to those obtained without applying mechanical

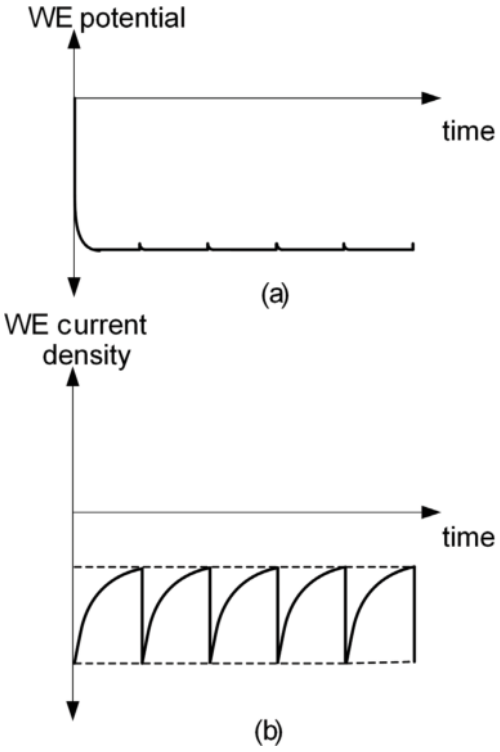

Figure 9. A graphic representation of electrodeposition signals versus time obtained during the electrodeposition process plus periodical mechanical perturbations: (a) WE potential and (b) WE current density [13].

http://dx.doi.org/10.5772/intechopen.78544

perturbations. Films were grown with two different thicknesses, 1200 and 500 nm, that were subjected to the annealing process. The morphology of the annealed films is shown in **Figure 10(c–f)**. In both cases, it is identified that the films are more compact when it is compared to the one obtained by not using mechanical perturbations during the electrodeposition process. As it can be seen on the micrographs, there is coalescence of grains along the film cross section, and the morphology is dense and crack free. Coalescence is achieved due to the fact that the composition is more homogeneous, zones with copper-poor and cooper-rich have been minimized, and the activation energy for grain growth is more uniform throughout the film. This film morphology is completely different from that obtained without applying mechanical perturbations, where there was only coalescence in the first 300 nm of thickness. This is because a more compact

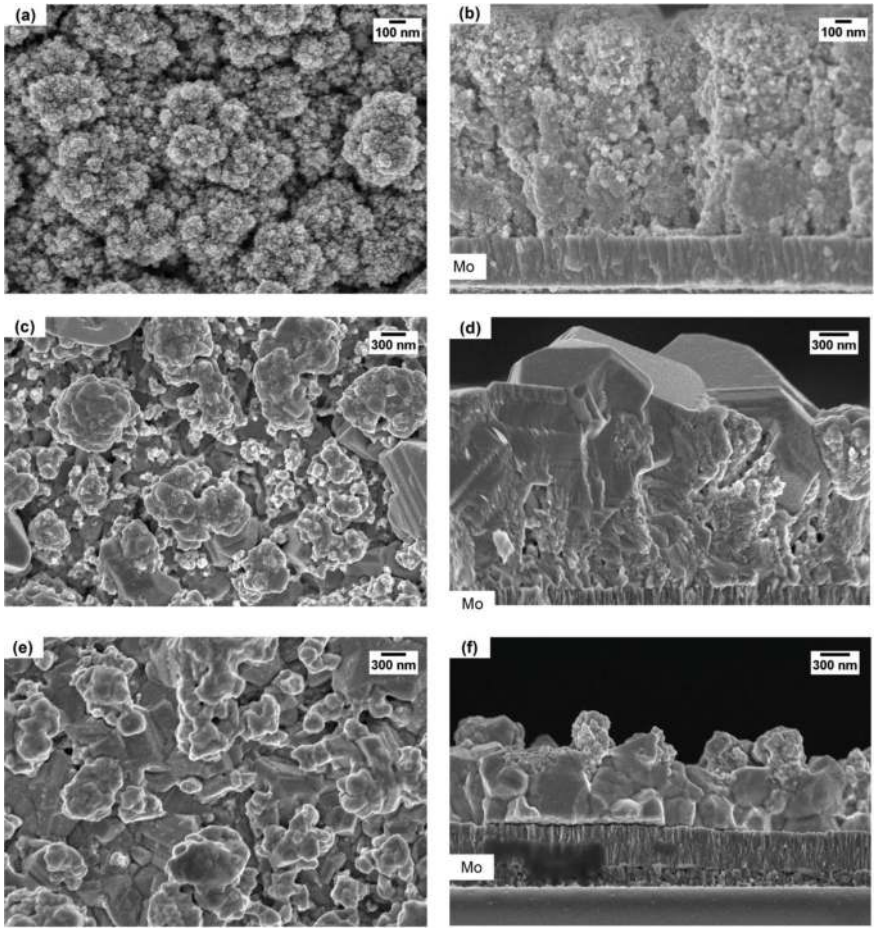

Figure 10. Micrographs of the surface and cross section of the films that have been grown in a potentiostatic mode with mechanical perturbations. (a,b) without annealing, (c,d) annealed films with a thickness of 1200 nm, and (e,f) annealed films with a thickness of 500 nm [13].

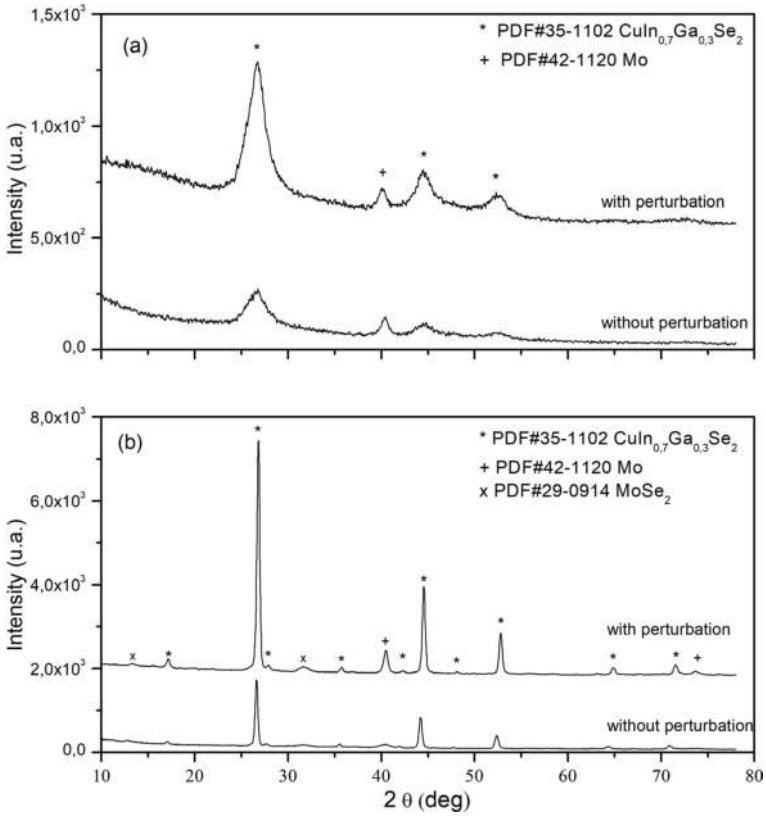

Figure 11. GIXRD diffraction pattern of CIGS films obtained with mechanical perturbation and without mechanical perturbation: (a) as-electrodeposited films and (b) annealed films [13].

morphology was obtained from the electrodeposition process with mechanical perturbations, and it represents a route for obtaining CIGS films by electrodeposition with improved morphology.

Figure 11 shows the GIXRD diffraction pattern for the film deposited with a potentiostatic mode with and without periodical mechanical perturbations with an incidence angle of 1.5°. The $CuIn_xGa_{(1-x)}Se_2$, Mo, and $MoSe_2$ structures are identified according to PDF#35–1102, PDF#42–1120, and PDF#29–0914. First of all, the films exhibit a highly (112) preferred orientation. From **Figure 11(a)**, it can be seen that the as-electrodeposited film shows a poor crystallinity, which is a characteristic of CIGS films before annealing. Also, a diffraction peak of the Mo, which is the substrate and back contact, is identified. The main difference in the diffraction patterns is that there is a greater intensity in the film formed with mechanical perturbation than the film formed without mechanical perturbation. This indicates the presence of higher crystallinity in the film obtained with the mechanical perturbation. **Figure 11(b)** presents the diffraction patterns of the annealed films in selenium atmosphere; these show a high crystalline quality, which is revealed by the well-defined chalcopyrite peaks. The annealing

process clearly increased the grain size, as indicated by the reduction of the peak full-width at half-maximum (FWHM). For the CIGS film formed without mechanical perturbation, the crystal size was 26.6 nm, and for the CIGS film formed with mechanical perturbation, the crystal size was 26.0 nm. This can be expected because the peaks of both films have FWHM that are alike. The annealed films, in a similar manner to the as-electrodeposited film, have a greater intensity in the diffraction peaks for the film formed with mechanical perturbation than for the film formed without mechanical perturbation. Probably, one of the reasons is that the films obtained with mechanical perturbation are denser. The results shown by XRD and SEM clearly demonstrate the advantages of applying periodic perturbations during the electrodeposition process, this being a new route to synthesize thin films.

6. Conclusion(s)

Employing periodic mechanical perturbations during the electrodeposition process allows a better distribution of ionic species on the working electrode surface. This methodology represents a novel approach for the fabrication of thin films by electrodeposition. This has been demonstrated successfully in the synthesis of compact CIGS thin films. It has the advantage to obtain a homogeneous morphology CIGS films in the as-electrodeposited films, as well, in the annealed film. In this strategy, there is no dissolution of the film during the electrodeposition process, as taking place in pulse-reverse electrodeposition. It is a route to obtain CIGS films by electrodeposition with compact morphology and large grains. Further studies should be done about the mechanical perturbation frequency and the effect on the solar cell efficiency.

Acknowledgements

This chapter was supported through the projets C16-FAI-09-58.58, PAPIIT-IN117216, CONACYT-82306 and CONACYT-UNAM (LIFYCS), specially with the use of ICP-AES ULTIMA 2 and SEM S-5500. Also, we would like to thank María Luis Ramón García for the XRD and Rogelio Morán Elvira fo SEM measurements.

Author details

Baudel Lara Lara[1]*, Arturo Fernández Madrigal[2], Lizbeth Morales Salas[2] and Alejandro Altamirano Gutiérrez[3]

*Address all correspondence to: ing_lara@uaslp.mx

1 Facultad de Ingeniería, Universidad Autónoma de San Luis Potosí, Zona Universitaria Poniente, San Luis Potosí, S. L. P., México

2 Instituto de Energías Renovables, Universidad Nacional Autónoma de México, Temixco, Morelos, México

3 Centro Universitario de Tonalá, Universidad de Guadalajara, Tonalá, Jalisco, México

References

[1] Bhattacharya RN. Solution growth and electrodeposited $CuInSe_2$ thin films. Journal of the Electrochemical Society. 1983;**130**:2040-2042. DOI: 10.1149/1.2119516

[2] Peter LM. Electrochemical routes to earth-abundant photovoltaics: A minireview. Electrochemistry Communications. 2015;**50**:88-92

[3] Chen H, Wei Z, Zheng X, Yang S. A scalable electrodeposition route to the low-cost, versatile and controllable fabrication of perovskite solar cells. Nano Energy. 2015;**15**:216-226

[4] Septina W, Ikeda S, Kyoraiseki A, Harada T, Matsumura M. Single-step electrodeposition of a microcrystalline $Cu_2ZnSnSe_4$ thin film with a kesterite structure. Electrochimica Acta. 2013;**88**:436-442

[5] Bhattacharya RN, Oh MK, Kim Y. CIGS-based solar cells prepared from electrodeposited precursor films. Solar Energy Materials and Solar Cells. 2012;**98**:198-202. DOI: 10.1016/j.solmat.2011.10.026

[6] Nady JE, Kashyout AB, Ebrahim S, Soliman MB. Nanoparticles Ni electroplating and black paint for solar collector applications. Alexandria Engineering Journal. 2016;**55**:723-729

[7] Wang J, Lei Z, Zhou Q, Wu W, Zhu C, Liu Z, Chang S, Pu J, Zhang H. Ultra-flexible lithium ion batteries fabricated by electrodeposition and solvothermal synthesis. Electrochimica Acta. 2017;**237**:119-126

[8] Budevski E, Staikov G, Lorenz WJ. Electrocrystallization nucleation and growth phenomena. Electrochimica Acta. 2000;**45**:2559-2574. DOI: 10.1016/S0013-4686(00)00353-4

[9] Taylor SR, Gileadi E. Physical interpretation of the Warburg impedance. Corrosion. 1995;**51**(9):664-671

[10] Fu Y-P, You R-W, Lew K-K. Electrochemical properties of solid–liquid interface of $CuIn_{1-x}Ga_xSe_2$ prepared by electrodeposition with various gallium concentrations. Journal of the Electrochemical Society. 2009;**156**(9):E133-E138. DOI: 10.1149/1.3158558

[11] Zahraei M, Saidi MS, Sani M. Numerical simulation of electro-deposition process influenced by force convection and migration of ions. Journal of Electroanalytical Chemistry. 2016;**782**:117-124. DOI: 10.1016/j.jelechem.2016.012

[12] Scharifker B, Hills G. Theoretical and experimental studies of multiple nucleation. Electrochimica Acta. 1983;**28**(7):879-889. DOI: 10.1016/0013-4686(83)85163-9

[13] Lara-Lara B, Fernández AM. CIGS this film growing by electrodeposition technique using mechanical perturbation at the working electrode. Journal of Materials Science: Materials in Electronics. 2016;**27**:5099-5106. DOI: 10.1007/s10854-016-4400-1

[14] Jackson P, Wuerz R, Hariskos D, Lotter E, Witte W, Powalla M. Effects of heavy alkali elements in cu(in,Ga)Se_2 solar cells with efficiencies up to 22.6%. Physica Status Solidi RRL: Rapid Research Letters. 2016;**10**(8):583-586. DOI: 10.1002/pssr.201600199

[15] Repins I, Contreras MA, Egaas B, DeHart C, Scharf J, Perkins CL, To B, Noufi R. 19·9%-efficient ZnO/CdS/CuInGaSe$_2$ solar cell with 81·2% fill factor. Progress in Photovoltaics: Research and Applications. 2008;**16**:235-239. DOI: 10.1002/pip.822

[16] Saji VS, Choi I-H, Lee C-W. Progress in electrodeposited absorber layer for CuIn$_{(1-x)}$Ga$_x$Se$_2$ (CIGS) solar cells. Solar Energy. 2011;**85**:2666-2678. DOI: 10.1016/j.solener.2011.08.003

[17] Hibberd CJ, Chassaing E, Liu W, Mitzi DB, Lincot D, Tiwari AN. Non-vacuum methods for formation of Cu(In,Ga)(Se,S)$_2$ thin film photovoltaic absorbers. Progress in Photovoltaics: Research and Applications. 2010;**18**:434-452. DOI: 10.1002/pip.914

[18] Lincot D, Guillemoles JF, Taunier S, Guimard D, Sicx-Kurdi J, Chaumont A, Roussel O, Ramdani O, Hubert C, Fauvarque JP, Bodereau N, Parissi L, Panheleux P, Fanouillere P, Naghavi N, Grand PP, Benfarah M, Mogensen P, Kerrec O. Chalcopyrite thin film solar cells by electrodeposition. Solar Energy. 2004;**77**:725-737. DOI: 10.1016/j.solener.2004.05.024

[19] Aksu S, Pinarbasi M. Electrodeposition methods and chemistries for deposition of CIGS precursor thin films. 37th IEEE Photovoltaic Specialists Conference (PVSC). 2011:310-314

[20] Bhattacharya RN, Fernández AM. CuIn$_{1-x}$Ga$_x$Se$_2$-based photovoltaic cells from electrodeposited precursors films. Solar Energy Materials & Solar Cells. 2003;**76**:331-337. DOI: 10.1016/S0927-0248(02)00285-4

[21] Dale P, Peter L. Applications of electrochemistry in the fabrication and characterization of thin-film solar cell. In: Alkire RC, Kolb DM, Lipkowski J, Ross PN, editors. Photoelectrochemical Materials and Energy Conversion Processes. Vol. 12. Wiley-VCH Verlag GmbH Co; 2011. DOI: 10.1002/9783527633227

[22] Roussel O, Ramdani O, Chassaing E, Grand P-P, Lamirand M, Etcheberry A, Kerrec O, Guillemoles J-F, Lincot D. First stages of CuInSe$_2$ electrodeposition from cu(II)-in(III)-se(IV) acidic solutions on polycrystalline Mo films. Journal of the Electrochemical Society. 2008;**155**. DOI: D141–D147. DOI: 10.1149/1.2815476

[23] Chassaing E, Grand P-P, Ramdani O, Vigneron J, Etcheberry A, Lincot D. Electrocrystallization mechanism of cu–in–se compounds for solar cell applications. Journal of the Electrochemical Society. 2010;**157**(7). DOI: D387–D395. DOI: 10.1149/1.3374590

[24] Huang H-C, Lin C-S, Chen F-J, Li W-C. Direct observation of the electrocrystallization of compound CuInSe$_2$ during the early stages of deposition. Electrochimica Acta. 2013;**97**:244-252

[25] Lai Y, Liu J, Yang J, Wang B, Liu F, Zhang Z, Li J, Liu Y. Incorporation mechanism of indium and gallium during electrodeposition of cu(in,Ga)Se$_2$ thin film. Journal of the Electrochemical Society. 2011;**158**. DOI: D704–D709. DOI: 10.1149/2.059112jes

[26] Sang ND, Quang PH, Tu LT, Hop DTB. Effect of electrodeposition potential on composition and morphology of CIGS absorber thin film. Bulletin of Materials Science. 2013;**36**:735-741. DOI: 10.1007/s12034-013-0497-5

[27] Fernández AM, Bhattacharya RN. Electrodeposition of $CuIn_{1-x}Ga_xSe_2$ precursor films: Optimization of film composition and morphology. Thin Solid Films. 2005;**474**:10-13. DOI: 10.1016/j.tsf.2004.02.104

[28] Liu J, Liu F, Lai Y, Zhang Z, Li J, Liu Y. Effects of sodium sulfamate on electrodeposition of cu(in,Ga)Se_2 thin film. Journal of Electroanalytical Chemistry. 2011;**651**:191-196. DOI: 10.1016/j.jelechem.2010.10.021

[29] Calixto ME, Dobson KD, McCandless BE, Birkmire RW. Controlling growth chemistry and morphology of single-bath electrodeposited cu(in,Ga)Se_2 thin films for photovoltaic application. Journal of the Electrochemical Society. 2005;**153**(6). DOI: G521–G528. DOI:10.1149/1.2186764

[30] Fu Y-P, You R-W, Lew KK. $CuIn_{1-x}Ga_xSe_2$ absorber layer fabricated by pulse-reverse electrodeposition technique for thin films solar cell. Journal of the Electrochemical Society. 2009;**156**(12):D553-D557. DOI: 10.1149/1.3240330

[31] Lara-Lara B, Fernández AM. Influence of electrode position in the electrolytic cell configuration for the electrodeposition of cu(in,Ga)Se_2 thin films. Journal of Materials Science: Materials in Electronics. 2015;**26**:5593-5560. DOI: 10.1007/s10854-014-2319-y

[32] Chirilă A, Reinhard P, Pianezzi F, Bloesch P, Uhl AR, Fella C, Kranz L, Keller D, Gretener C, Hagendorfer H, Jaeger D, Erni R, Nishiwaki S, Buecheler S, Tiwari AN. Potassium-induced surface modification of cu(in,Ga)Se_2 thin films for high-efficiency solar cells. Nature Materials. 2013;**12**:1107-1111. DOI: 10.1038/nmat3789

[33] Jackson P, Hariskos D, Lotter E, Paetel S, Wuerz R, Menner R, Wischmann W, Powalla M. New world record efficiency for cu(in,Ga)Se_2 thin-film solar cells beyond 20%. Progress in Photovoltaics: Research and Applications. 2011;**19**:894-897. DOI: 10.1002/pip.1078

[34] Gamburg YD, Zangari G. Theory and Practice of Metal Electrodeposition. New York: Springer; 2011. DOI: 10.1007/978-1-4419-9669-5_1

[35] Kampmann A, Sittinger V, Rechid J, Reineke-Koch R. Large area electrodeposition of cu(in,Ga)Se_2. Thin Solid Films. 2000. DOI: 361-362:309-313. DOI:10.1016/S0040-6090(99)00863-9

[36] Schlenker T, Valero ML, Schock HW, Werner JH. Grain growth studies of thin cu(in, Ga)Se_2 films. Journal of Crystal Growth. 2004;**264**:178-183. DOI: 10.1016/j.jcrysgro.2004.01.020

[37] You R-W, Lew KK, Fu Y-P. Effect of indium concentration on electrochemical properties of electrode-electrolyte interface of $CuIn_{1-x}Ga_xSe_2$ prepared by electrodeposition. Materials Research Bulletin. 2017;**96**:183-187. DOI: 10.1016/j.materresbull.2017.04.027